

Supporting Information

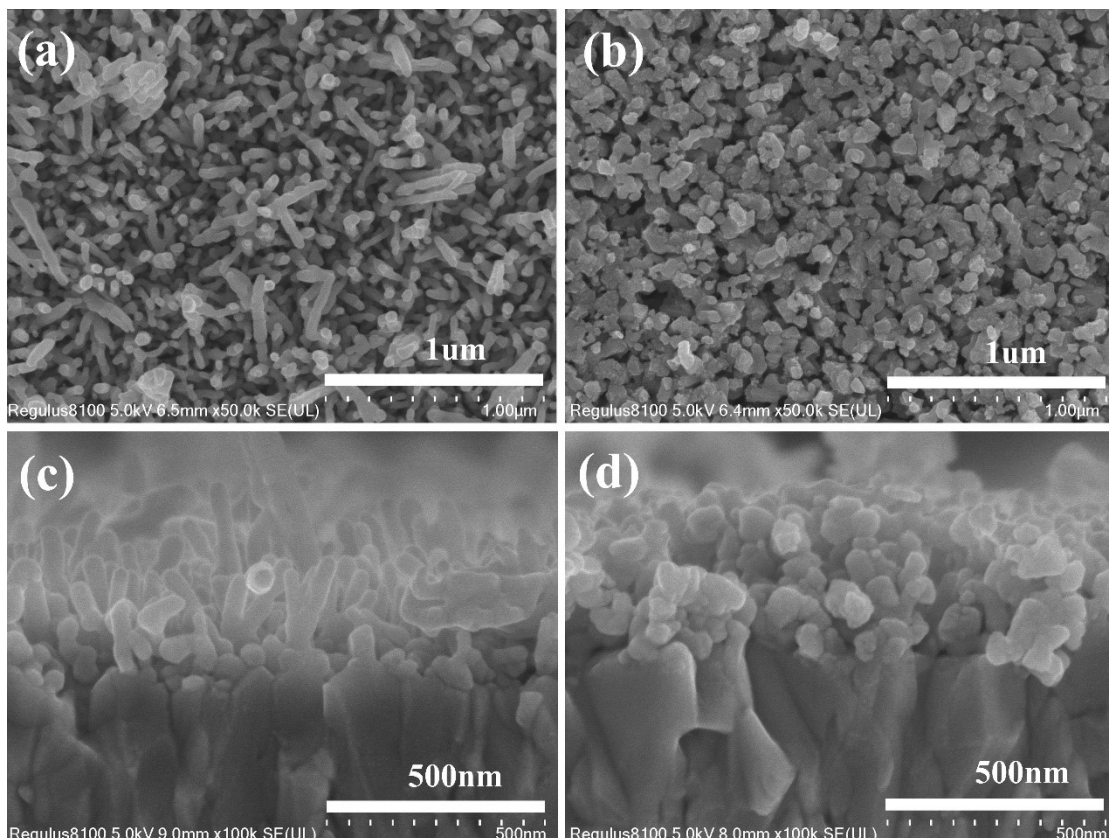


Figure S1: (a) and (b) Top-view SEM images of $\text{Fe}_2\text{O}_3/\text{g-C}_3\text{N}_4$ -1 and $\text{Fe}_2\text{O}_3/\text{g-C}_3\text{N}_4$ -3 (c),(d) Cross-sectional electron microscopy (SEM) images of $\text{Fe}_2\text{O}_3/\text{g-C}_3\text{N}_4$ -1 and $\text{Fe}_2\text{O}_3/\text{g-C}_3\text{N}_4$ -3

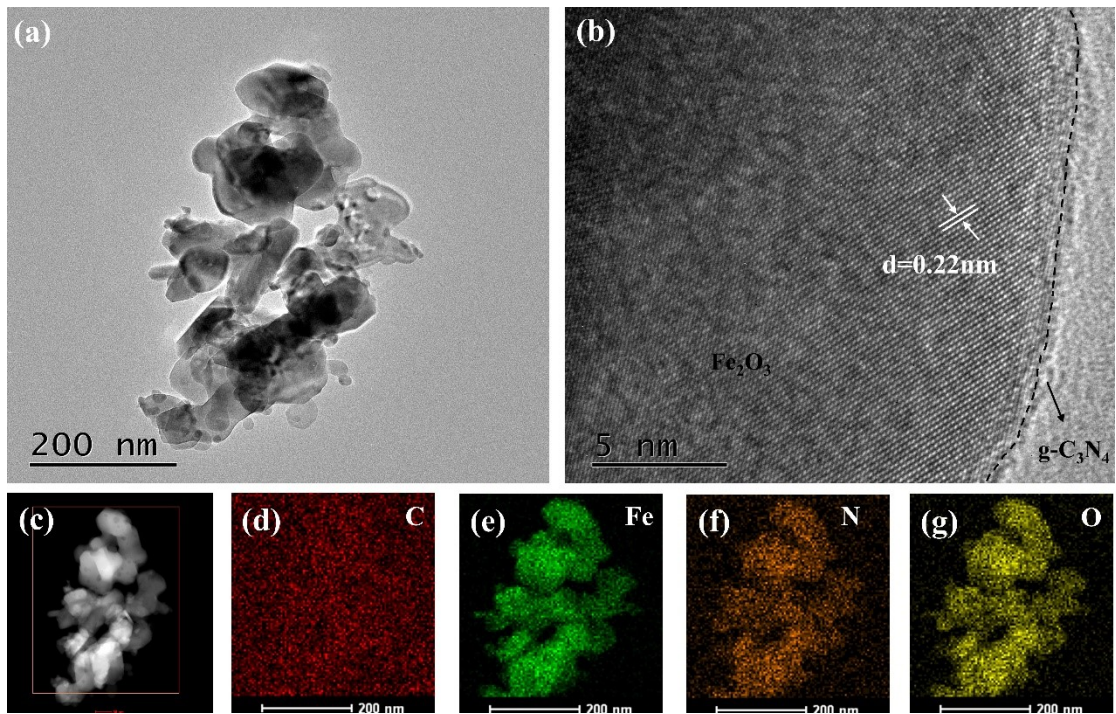


Figure S2: (a)The transmission electron microscope images (TEM) of $\text{Fe}_2\text{O}_3/\text{g-C}_3\text{N}_4$ -2 (b)The high-resolution transmission electron microscopy image of $\text{Fe}_2\text{O}_3/\text{g-C}_3\text{N}_4$ -2; (c)TEM image in dark-field mode of $\text{Fe}_2\text{O}_3/\text{g-C}_3\text{N}_4$ -2; (d-g) The element mapping images of C、Fe、N、O

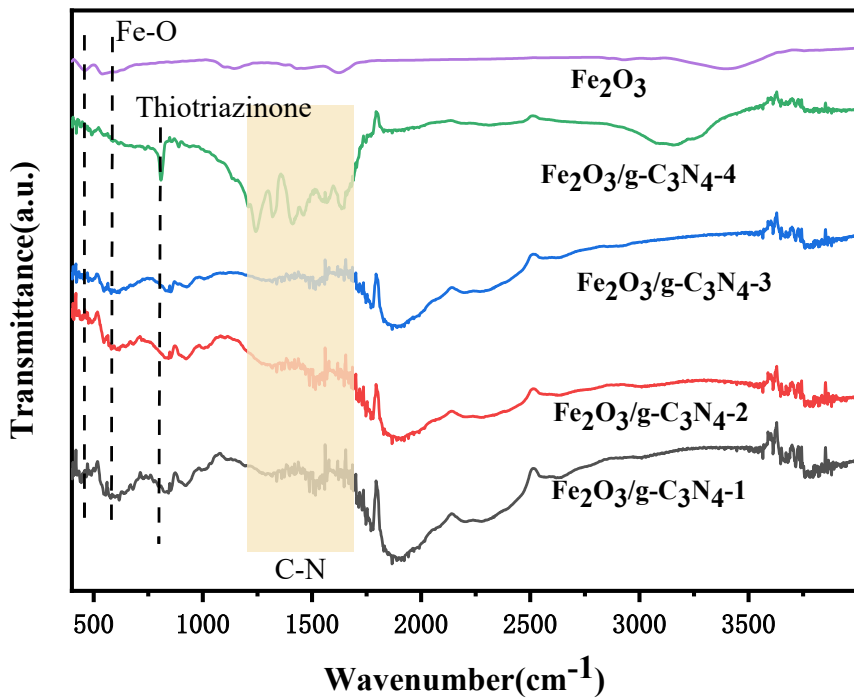


Figure S3: Fourier transform infrared spectra of Fe_2O_3 、 $\text{Fe}_2\text{O}_3/\text{g-C}_3\text{N}_4$ -1、 $\text{Fe}_2\text{O}_3/\text{g-C}_3\text{N}_4$ -2、 $\text{Fe}_2\text{O}_3/\text{g-C}_3\text{N}_4$ -3 and $\text{Fe}_2\text{O}_3/\text{g-C}_3\text{N}_4$ -4